REPORT

WNT1 Mutations in Families Affected by Moderately Severe and Progressive Recessive Osteogenesis Imperfecta

Shawna M. Pyott,[1,*] Thao T. Tran,[1] Dru F. Leistritz,[1] Melanie G. Pepin,[1] Nancy J. Mendelsohn,[2,3] Renee T. Temme,[2] Bridget A. Fernandez,[4] Solaf M. Elsayed,[5] Ezzat Elsobky,[5] Ishwar Verma,[6] Sreelata Nair,[7] Emily H. Turner,[8] Joshua D. Smith,[8] Gail P. Jarvik,[9] and Peter H. Byers[1,9]

Osteogenesis imperfecta (OI) is a heritable disorder that ranges in severity from death in the perinatal period to an increased lifetime risk of fracture. Mutations in *COL1A1* and *COL1A2*, which encode the chains of type I procollagen, result in dominant forms of OI, and mutations in several other genes result in recessive forms of OI. Here, we describe four recessive-OI-affected families in which we identified causative mutations in wingless-type MMTV integration site family 1 (*WNT1*). In family 1, we identified a homozygous missense mutation by exome sequencing. In family 2, we identified a homozygous nonsense mutation predicted to produce truncated WNT1. In family 3, we found a nonsense mutation and a single-nucleotide duplication on different alleles, and in family 4, we found a homozygous 14 bp deletion. The mutations in families 3 and 4 are predicted to result in nonsense-mediated mRNA decay and the absence of WNT1. WNT1 is a secreted signaling protein that binds the frizzled receptor (FZD) and the coreceptor low-density lipoprotein-receptor-related protein 5 (LRP5). Biallelic loss-of-function mutations in *LRP5* result in recessive osteoporosis-pseudoglioma syndrome with low bone mass, whereas heterozygous gain-of-function mutations result in van Buchem disease with elevated bone density. Biallelic loss-of-function mutations in *WNT1* result in a recessive clinical picture that includes bone fragility with a moderately severe and progressive presentation that is not easily distinguished from dominant OI type III.

In most populations, more than 95% of individuals with osteogenesis imperfecta (OI [MIM 166200, 166210, 259420, and 166220]) have dominant mutations in the type I collagen genes, *COL1A1* (MIM 120150) and *COL1A2* (MIM 120160). Recessively inherited forms of OI (MIM 613849, 610682, 610915, 259440, 613848, 610968, 613982, 614856, and 615066) account for most of the remainder. These phenotypes can result from mutations in (1) genes important for osteoblast differentiation (*SP7*[1] [MIM 606633]), (2) genes encoding proteins that modify collagens or act as chaperones during assembly and secretion of collagens (*CRTAP*[2,3] [MIM 605497], *LEPRE1*[4,5] [MIM 610339], *PPIB*[6–8] [MIM 123841], *SERPINH1*[9] [MIM 600943], *FKBP10*[10,11] [MIM 607063], *SERPINF1*[12,13] [MIM 172860], and *BMP1*[14,15] [MIM 112264]), or (3) genes that modulate intracellular calcium levels (*TMEM38B*[16] [MIM 611236]). Most laboratories that study OI have seen affected families in which the molecular basis remains unsolved. We used exome sequence analysis[17] to identify a homozygous *WNT1* mutation in one family and then screened 37 additional probands with moderate to lethal OI (mutations in *COL1A1*, *COL1A2*, and other genes previously linked to recessive forms of OI had previously been excluded, and these individuals had normal mobility of type I collagen as detected by polyacrylamide-gel electrophoresis). All samples were collected according to the guidelines of the University of Washington institutional review board, and proper informed consent was obtained. Among the 37 additional probands, we identified three families affected by biallelic *WNT1* mutations that led to moderately severe and progressive forms of OI.

Exome sequence analysis was done by the Northwest Genomics Center at the University of Washington with DNA from two adult siblings, the proband (IV-2) and the unaffected sister (IV-4), from family 1 (Figure 1A). In brief, genomic DNA was extracted from blood and 1 μg was subjected to a series of library-construction steps, including fragmentation through acoustic sonication (Covaris), end polishing and A tailing, ligation of sequencing adaptors, and PCR amplification with 8 bp barcodes for multiplexing. Exome capture was done with the ~36.5 Mb target from Roche Nimblegen SeqCap EZ v.2.0 (~300,000 exons and flanking sequence). The barcoded exome libraries were pooled, and then massively parallel sequencing by synthesis with fluorescently labeled, reversibly terminating nucleotides was carried out on a HiSeq machine. The demultiplexed BAM files were aligned to a human reference (UCSC Genome Browser hg19) with Burrows-Wheeler Aligner v.0.5.9.[18] Read pairs not mapping within ± 2 SDs of the average library size (~125 ± 15 bp for exomes) were removed. Aligned read data were edited by duplicate removal (i.e., the removal of reads with duplicate start positions; Picard MarkDuplicates; v.1.14), indel

[1]Department of Pathology, University of Washington, Seattle, WA 98195-7470, USA; [2]Medical Genetics Division, Children's Hospitals and Clinics of Minnesota, Minneapolis, MN 55404, USA; [3]Division of Genetics, Department of Pediatrics, University of Minnesota, Minneapolis, MN 55454, USA; [4]Disciplines of Genetics and Medicine, Memorial University of Newfoundland, St. John's NL A1B 3V6, Canada; [5]Genetics Unit, Pediatrics Department, Ain Shams University, Cairo 11566, Egypt; [6]Department of Medical Genetics, Sir Ganga Ram Hospital, New Delhi 110060, India; [7]Fetal Medicine and Genetics Department, Lifeline Super Specialty Hospital, Kerala 691523, India; [8]Department of Genome Sciences, University of Washington, Seattle, WA 98195-5065, USA; [9]Division of Medical Genetics, Department of Medicine, University of Washington, Seattle, WA 98195-7470, USA
*Correspondence: shawnap@uw.edu
http://dx.doi.org/10.1016/j.ajhg.2013.02.009.

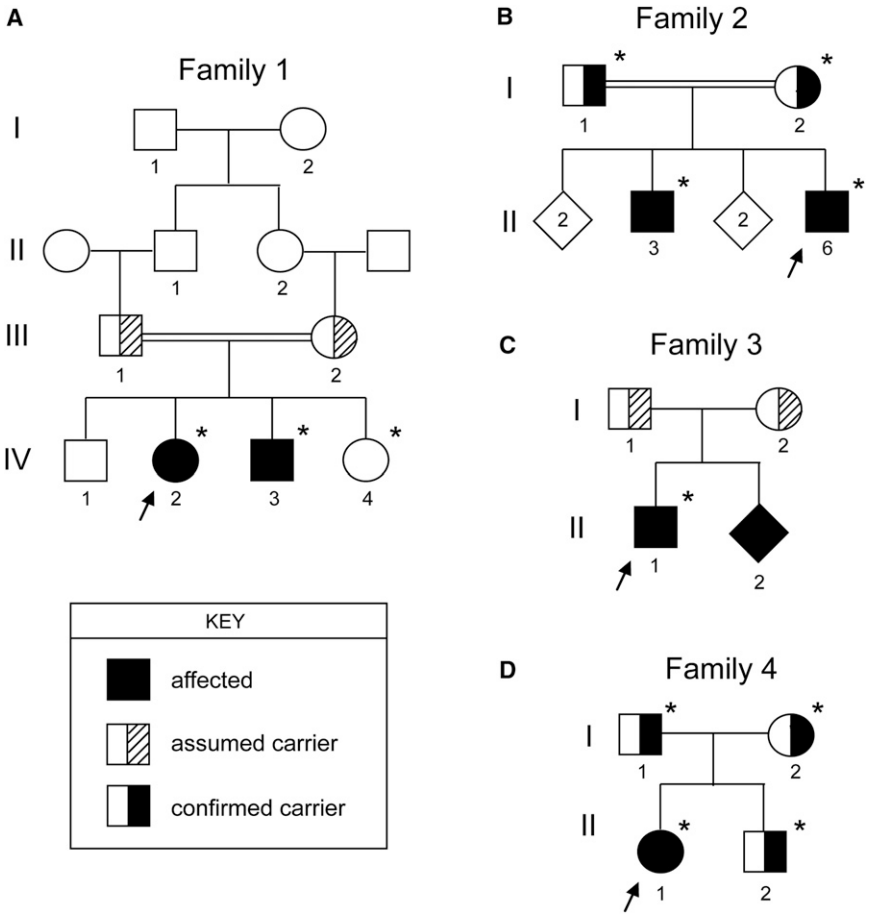

Figure 1. Pedigrees of the Families Affected by *WNT1* Mutations
Families 1 (A), 2 (B), 3 (C), and 4 (D). For family 1, exome sequences were determined for individuals IV-2 and IV-4. Arrows indicate the proband from each family, and the asterisks indicate the individuals studied from each family.

realignment was performed (GATK IndelRealigner; v.1.0-6125), and base qualities were recalibrated (GATK TableRecalibration; v.1.0-6125). Variant detection and genotyping were performed with the UnifiedGenotyper tool from GATK (v.1.0-6125). The SeattleSeq Annotation Server was used for annotating variants for providing dbSNP reference SNP IDs, gene names and accession numbers, the predicted functional effect (e.g., splice-site, nonsynonymous, missense, etc.), protein positions and amino acid changes, PolyPhen predictions, conservation scores (e.g., PhastCons and Genomic Evolutionary Rate Profiling), the ancestral allele, dbSNP allele frequencies, and known clinical associations. After this procedure, the data set for the two adult siblings (IV-2 and IV-4) in family 1 contained approximately 17,000 variants. Removal of all intergenic and intronic variants, variants present in dbSNP, or variants represented greater than ten times in the National Heart, Lung, and Blood Institute (NHLBI) Exome Sequencing Project Exome Variant Server (EVS) reduced the list to 2,400. When only variants that were homozygous in the proband and heterozygous or homozygous at the same site for a different nucleotide were considered, the number of variants for consideration was reduced to 17. In the proband, this group consisted of nine coding synonymous changes, a 14 bp deletion, six missense changes, and a variant within the 5′ UTR of a gene. None of the coding synonymous changes appeared to alter splice enhancer or suppressor sequences and were therefore not considered further. Variants with a low conservation score were discarded. The remaining five candidate genes were *OR4Q3*, *WNT1* (MIM 164820), *NAV3* (MIM 611629), *OTOGL* (MIM 614925), and *CELA3A*. Because biallelic loss-of-function mutations in low-density lipoprotein-receptor-related protein 5 (*LRP5* [MIM 603506]), which encodes a coreceptor of WNT1, result in recessive osteoporosis-pseudoglioma syndrome (OPPG [MIM 259770]) with low bone mass and because heterozygous gain-of-function mutations result in dominantly inherited van Buchem disease, type 2 (MIM 607636) (also known as endosteal hyperostosis) with elevated bone density, *WNT1* was the best candidate gene. The proband (IV-2 in family 1) was homozygous for a missense mutation (c.893T>G [p.Phe298Cys]) in *WNT1* (RefSeq accession number NM_005430.3), and the unaffected sibling (IV-4) was homozygous for the wild-type allele.

The proband (IV-2) had her first recognized fracture (femur) at the age of 2 years after mild trauma when she started to walk. Radiography at the time revealed a healed fracture of her humerus, but this had not been noted clinically. The diagnosis of OI was reached after several additional fractures and progressive long-bone deformity. She had blue sclera, her teeth were normal, her hearing was normal, and her intellectual function was normal (she was a high school graduate). Studies of dual energy X-ray absorptiometry were not done. Her younger brother (IV-3) had fractures that began at the age of 1 year and developed more severe deformity. He had normal teeth, normal hearing, and normal intellectual function (he was a college graduate). His scleral hue was not noted. Both individuals were treated surgically for the correction of deformities. Neither was treated with bisphosphonates. Radiographs taken when the individuals were in their late 20s showed a dramatic decrease in bone density and very marked deformity and shortening of long bones with striking scoliosis (Figure 2A); no other clinical

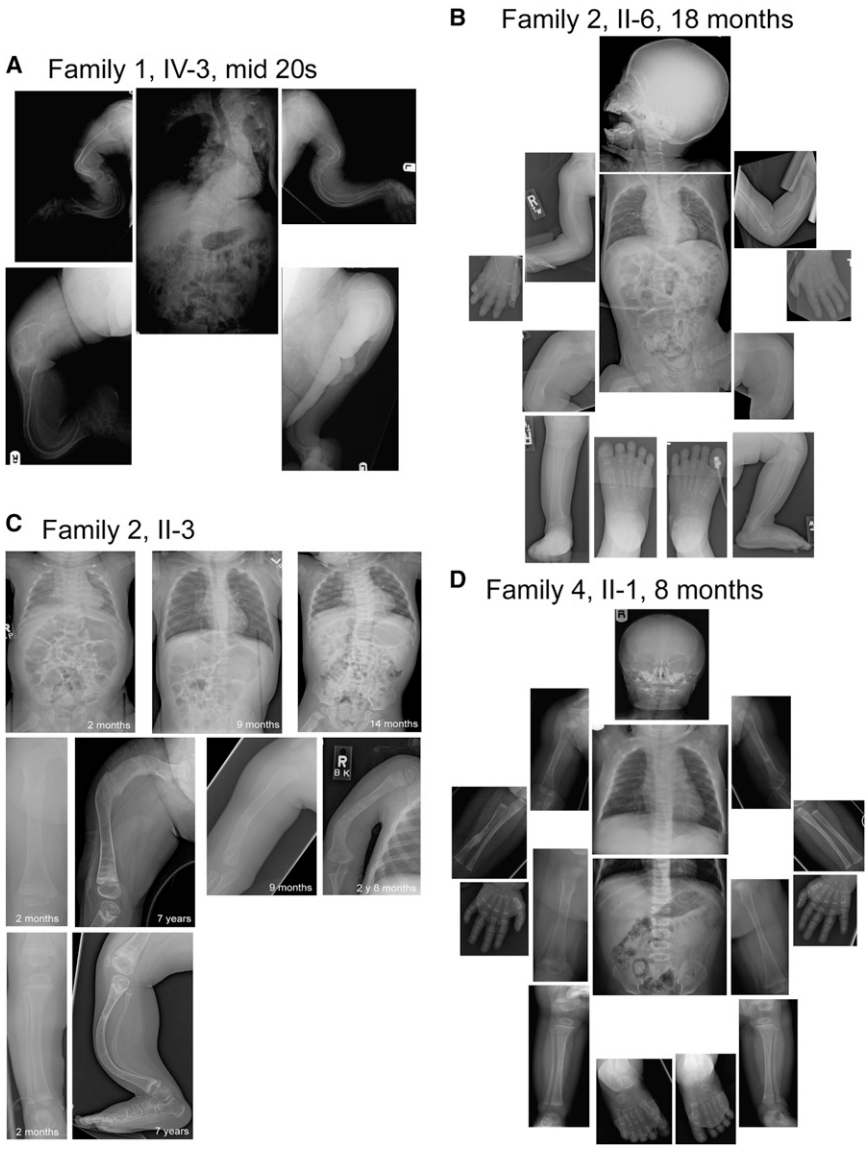

Figure 2. Radiographs of Affected Individuals with *WNT1* Mutations
(A) Radiographs taken in the mid 20s of individual IV-3 in family 1. There is marked bowing of the long bones in each extremity, low bone density, and striking scoliosis of the spine.
(B) Radiographs taken when II-6 (proband) from family 2 was 18 months of age show diminished mineralization of all long bones, bowing of several long bones, very marked bilateral angulation of the proximal femur, thin ribs, diminished calvarial mineralization, lack of bone modeling, and scoliosis.
(C) In radiographs taken of individual II-3 from family 2, the progression of scoliosis over the first year of life is apparent. There is marked change in bone structure and an increase in femoral bowing over 7 years.
(D) At the age of 7 months, individual II-1 from family 4 has decreased bone mineralization, platyspondyly, almost absent calvarial mineralization, but maintenance of long-bone structure with the exception of the fracture in the right radius.

information was available. Capillary sequencing (primers are available upon request) confirmed the exome sequence analysis in IV-2 and IV-4 and identified the homozygous c.893T>G mutation in the other affected sibling (IV-3 in family 1) (Figures 3A and 3B). Parental samples were not available for analysis.

Family 2 is of Hmong origin, and the proband (Figure 1B) has a clinical picture of severe OI. Both affected individuals (II-3 and II-6) are homozygous for a nonsense mutation (c.884C>A [p.Ser295*]) (Figures 3A and 3B) within the last exon of *WNT1*; this mutation results in stable mRNA (data not shown) and is predicted to result in a truncated protein. The same mutation has been identified in another Hmong family by an independent group and will be reported (Brendan Lee, personal communication). The father (I-1) and mother (I-2) are carriers of the mutation. Cultured fibroblasts from the proband (II-6) synthesized and secreted type I procollagen normally (data not shown). Although mRNA could be identified at a level similar to that in control fibroblasts, WNT1 was not at detectable levels in cells from either the proband or a control. As a consequence, we could not assess protein stability in cultured dermal fibroblasts.

The proband (II-6) is the sixth child born to first-cousin parents and is the second affected child within the sibship. Antenatally, a concern was raised about a brain malformation. He had a right humeral fracture at birth. When he was 14 months of age, an MRI of his brain revealed right unilateral cerebellar hypoplasia with congenital absence of the vermis, pontine hypoplasia, and hypoplasia of the mesencephalic tectum. The supratentorial anomalies included a small anterior commissure, hypoplasia of the optic chiasm and the hypothalamus, and closed-lip schizencephaly in the parasagittal region of the left occipital lobe. At 17 months of age, the proband was brought to the Children's Hospital and Clinics of Minnesota because of concerns about failure to thrive, developmental delays, and multiple fractures. At that time, he could hold his head up but had not met other significant developmental milestones. The baby was hospitalized for failure to thrive and was found to have feeding dysfunction that required a gastrostomy tube.

When he was 18 months old, his length was 75 cm (Z score = −2), his weight was 8.06 kg (Z score = −3.46), and his head circumference was 45.5 cm (fifth percentile). He was nondysmorphic in appearance, had normal teeth, and had normal scleral hue. The right humerus and both

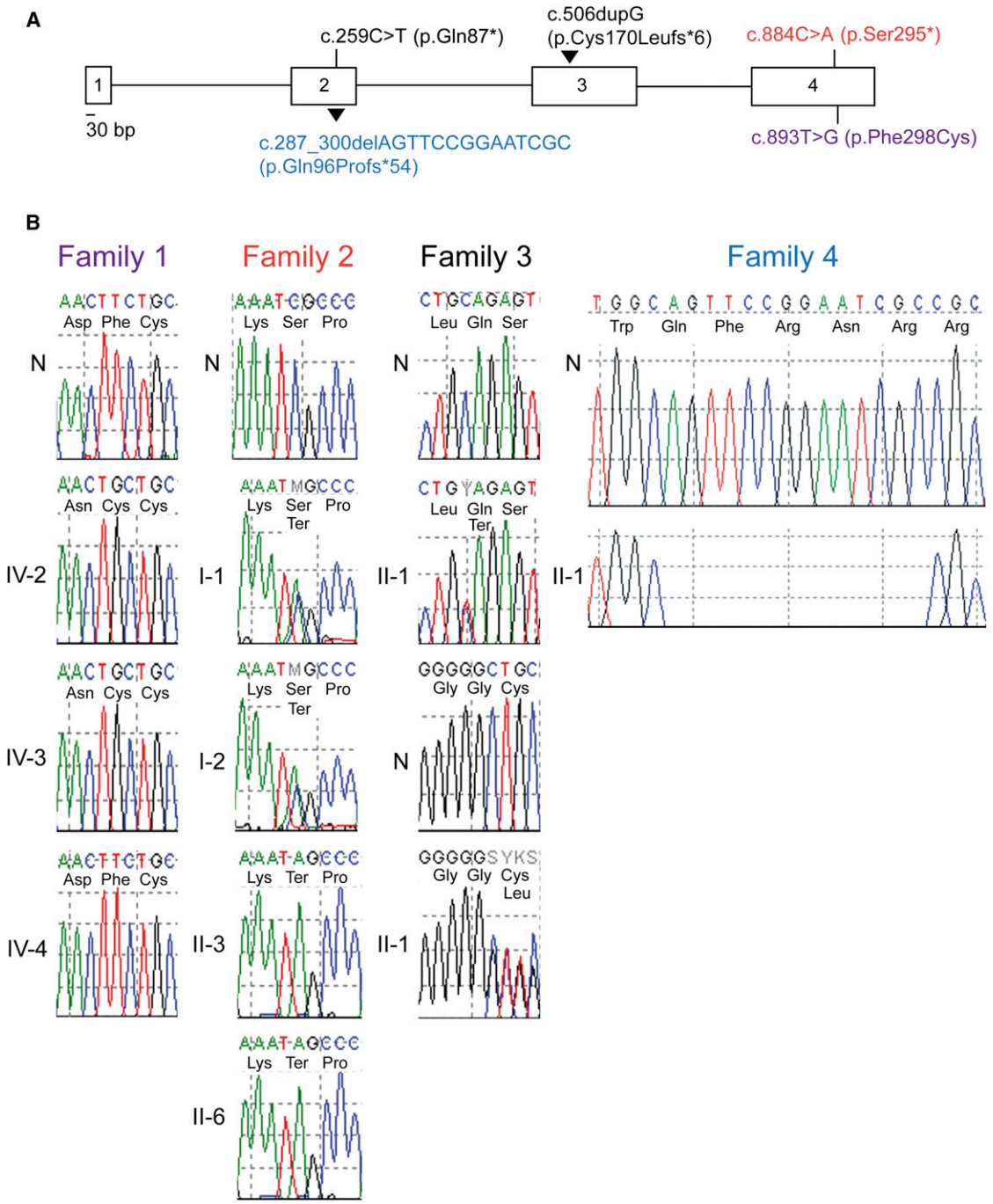

Figure 3. *WNT1* Mutations in Each Family
(A) Exon-intron structure and mutations in *WNT1* in four families. Color coding is as follows: purple, family 1; red, family 2; black, family 3; and blue, family 4.
(B) Sequence images of mutations in each family. Chromatograms labeled with N represent the normal reference sequence.

femurs were bowed (Figure 2B). He did not visually track or engage with the mother. Laboratory results within the reference range included creatine kinase, calcium, albumin, total serum protein, vitamin D, alkaline phosphatase, alanine transaminase, aspartate transaminase, free T4, thyroid-stimulating hormone, and parathyroid hormone. A skeletal survey showed several lambdoid intrasutural bones. There were multiple flattened vertebral bodies throughout the thoracic and upper lumbar spine. There were multiple fractures noted within the extremities, bowing at sites of healing, and areas of periosteal reaction. The healing fractures of both femoral diaphyses were associated with conspicuous apex anterior bowing.

The older affected brother (II-3) was born at 38 weeks of gestation and is the third child born to his healthy parents. At 3 hr of age, he was recognized to have a transverse

fracture of his left humerus, and at 10 days of age, he had a fracture of his right humerus. The first skeletal survey was taken when he was 2 months old and showed multiple extremity fractures, vertebral body compression, wormian bones, and generalized demineralization. Subsequently, several fractures occurred with resultant bone deformities. He has been treated with intermittent pamidronate infusion since he was 2 years old. Radiographs taken when he was 2 months, 9 months, and 14 months old show the progression of scoliosis (Figure 2C). He had marked bowing and deformity of the femurs by age 7 years. Developmentally, he has significant delays and a diagnosis of autism. At age 7 years, he had normal scleral hue and normal vision. He had developed self-injurious behavior, had no words or verbal skills, and had no way to directly indicate his needs. An MRI of his brain was normal. He was unable to walk but did command crawl and rolls easily. Measures of bone mineral density in both carrier parents were normal.

The affected individual (II-1) in family 3 (Figure 1C) has two mutations (c.506dupG [p.Cys170Leufs*6] and c.259C>T [p.Gln87*]) (Figures 3A and 3B), which were shown to be on different alleles by allele-specific amplification (data not shown). Both are predicted to lead to unstable mRNAs. The DNA for this study was extracted from a blood sample obtained when the child was 1 year and 9 months of age. At that time, there was a history of multiple fractures, poor feeding, delayed development, and recurrent infections. He had ptosis, could not hold his head up, and had a high arched palate. A computed-tomography scan showed thinning of the left temporal bone, and the referring physician thought that the child had a severe form of OI. The X-rays were not available to us to confirm these findings. Neither fibroblasts from the proband nor parental samples were available for study, and the clinical outcome of the child is unknown at this time.

Family 4 is from an isolated population in Newfoundland. The proband is homozygous for a deletion leading to a frameshift and premature termination codon (c.287_300delAGTTCCGGAATCGC [p.Gln96Profs*54]) (Figures 3A and 3B). The mutation is predicted to result in unstable mRNA as a result of nonsense-mediated decay and thus lead to the absence of WNT1. The father (I-1), mother (I-2), and brother (II-2) are all confirmed carriers.

At the age of 5 weeks, the female proband presented with a right humeral fracture. Skeletal survey showed multiple fractures—including those of the left humerus, the right seventh rib, and three metatarsals—that were thought to be 2–3 weeks old. There was osteopenia and compression of several lumbar vertebrae. At the age of 8 months, she began regular intravenous bisphosphonate infusions but continued to fracture. When she was 2 years old, intramedullary (IM) nails were placed in both femurs and tibiae. When she was 3 years and 9 months old, the distal portion of the left tibial nail erupted through the cortex and became subcutaneous and was replaced by an expansile nail.

When she was 13 months old, a brain MRI showed a type 1 Chiari malformation with 2 cm of tonsillar descent, which has been managed conservatively. The proband was born with right ptosis, which was repaired when she was 2 years old. When she was 2.5 years old, her parents became concerned about her development when they noticed crowd aversion and sound hypersensitivity. She started using single words just after her second birthday and joined words just before her third birthday. At 3 years of age, she was diagnosed with autism spectrum disorder and started receiving applied-behavioral-analysis therapy at home. By the age of 3 years and 5 months, she spoke in sentences.

On examination at age 3 years and 5 months, her height was 84.5 cm (less than the fifth percentile), her weight was 10.9 kg (less than the fifth percentile), and her head circumference was 48 cm (+1 SD). She had mild residual right ptosis and no other dysmorphic facial features. Her hands and feet were small: total hand length was 9.6 cm, and total foot length was 12.1 cm (both less than the third percentile).

WNT proteins are characterized by a set of 22 conserved cysteine residues that form the intrachain disulfide bridges that maintain the tertiary protein structure. WNT proteins are N-glycosylated and are acylated by the addition of palmitate and/or palmitoleic acid at a single serine residue (p.Ser224 in WNT1).[19] Acylation is required for the intracellular trafficking and full activity of the protein when secreted.[20] Recently, the crystal structure of a complex including *Xenopus* Wnt8 (xWnt8) bound to the cysteine-rich domain (CRD) of the mouse frizzled8 receptor (Fz8) was determined.[19] xWnt8 has a two-domain structure with "thumb" and "index-finger" extensions that interact with the Fz8-CRD domain. The carboxy-terminal domain (CTD) "index finger" has two β sheets maintained by six disulfide bridges, and the amino-terminal domain (NTD) "thumb" consists of a cluster of α helices stabilized by five disulfide bridges. The thumb extension at the NTD contains the palmitoleic acid residue that appears to interact with the hydrophobic groove of the Fz8 CRD, and the index-finger extension at the CTD also shows multiple contacts with hydrophobic regions of Fz8.

Placement of the human *WNT1* mutations on this model provides some insight into the mechanisms we might expect. The family 2 mutation (c.884C>A [p.Ser295*]) introduces a stop codon within the last exon (exon 4). In cultured fibroblasts, we found a stable mRNA (data not shown). A truncated protein that lacks 11 of 22 conserved cysteine residues and eliminates the entire CTD of the protein would be encoded by the mRNA. We could not determine whether the protein would be stable, but if it would, interaction with hydrophobic domains of the receptor would be ablated. In family 3 (see Figure 1C), the affected individual (II-1) is a compound heterozygote for two mutations (c.506dupG [p.Cys170 Leufs*6] and c.259C>T [p.Gln87*]), and in family 4, a 14 bp deletion (c.287_300delAGTTCCGGAATCGC

[p.Gln96Profs*54]) was identified. These mutations are predicted to generate unstable mRNAs, which would be targeted for nonsense-mediated decay and result in the absence of WNT1. The missense mutation in family 1 (c.893T>G [p.Phe298Cys] in the last exon) changes a phenylalanine residue at position 298 to a cysteine residue within the CTD of WNT1. In other WNT proteins, the equivalent 298 position tolerates either a hydrophobic (phenylalanine) or a polar (tyrosine) amino acid, but in either case, the adjacent residue is a conserved cysteine. The change to cysteine at position 298 introduces a tandem cysteine-cysteine set (of which two occur naturally) into the protein structure. The other two cysteine sets are also within the CTD, and the most C-terminal set was shown to be involved in an unusual tandem disulfide bond.[19] It is not clear what effect a third cysteine set would induce, but given the highly conserved nature of the cysteine residues in all WNT proteins, the change is likely to have a deleterious effect.

The pathway from mutations in *WNT1* to the OI phenotype is not yet clear. WNT1 interacts with two transmembrane receptor proteins, the frizzled receptor (FZD) and the coreceptor LRP5. Through these interactions, WNT1 regulates the canonical Wnt pathway through the phosphorylation of cytoplasmic β-catenin.[21,22] Upon interaction of WNT1 with the receptor complex, β-catenin is released from a degradation complex in the cytoplasm and translocated to the nucleus, where it interacts with the transcription factor TCF/LEF, and targeted gene expression is modulated. *SP7* (which encodes a transcription factor required for osteoblast differentiation and bone formation) and *ALPL* (MIM 171760) (which encodes tissue-nonspecific alkaline phosphatase that is key to bone mineralization) are among the downstream targets of Wnt signaling.[23,24] A homozygous mutation in *SP7* was identified in a child who has an OI type III–IV clinical picture and who was born into a consanguineous Egyptian family.[1] The mutation is predicted to alter DNA-binding properties of the encoded protein, osterix, and is thus thought to affect the expression of the downstream bone-related genes and osteoblast differentiation. Alterations in WNT1 signaling might thus alter *SP7* expression and result in similar downstream effects.

The canonical Wnt signaling pathway was recognized to play a role in bone formation and maintenance when homozygous loss-of-function mutations in *LRP5*, which encodes a coreceptor of WNT, were found to cause OPPG.[25] There are no reports of pseudoglioma in any of our affected individuals. In situ studies have shown that *Lrp5* is expressed in mouse osteoblasts and that the expression pattern of *Lrp5* changes over time in vitro as pluripotent mesenchymal cells are induced by Wnt-mediated signaling toward differentiation along the osteoblastic lineage. In addition, WNT-induced LRP5 signaling is necessary for the induction of alkaline phosphatase, a marker for mature osteoblasts, which places LRP5 and WNT together in the cell-differentiation pathway. Interestingly, family members heterozygous for the *LRP5* loss-of-function mutations were found to have lower bone mineral density than were the age- and gender-matched controls.[25]

In mice homozygous for mutations in both *Lrp5* and *Lrp6*, documented osteoblast proliferation was defective, so this pathway is another downstream target of Wnt signaling. In humans, heterozygous missense (gain-of-function) mutations in *LRP5* result in van Buchem disease type 2 (endosteal hyperostosis) with elevated bone density,[26,27] and equivalent mutations in mice recapitulate the human high-bone-mass phenotype.[28]

In mesenchymal stem cells, Wnt proteins play a role in sustaining stem cell self-renewal and differentiation potential,[29,30] and there is evidence that Wnt signaling in osteocytes is required for normal bone homeostasis.[31] The studies of mutations in *LRP5*, outlined above, place the canonical Wnt pathway in the early stages of bone development and suggest, in addition, that it has a role during osteoblast differentiation and proliferation. Given the tight regulation between osteoblasts and osteoclasts during skeletal development,[32] perhaps both cell types are downstream targets of Wnt signaling. *Wnt1*-knockout mice[33] die in the neonatal period with virtually no midbrain and no cerebellum, whereas the naturally occurring *Wnt1* mutant "swaying" mice[34] (with c.565delG [p.Glu189Argfs*10]) live to adulthood and are characterized by ataxia and hypertonia, a phenotype attributed to the malformation of the anterior regions of the cerebellum. This mutation is similar to the one that we identified in family 3. Given that neither mouse model describes a bone phenotype, insight regarding the effect of altered WNT1 function on bone development is lacking. The cerebellar malformations seen in the mouse models were not seen in our four families affected by human *WNT1* mutations, which suggests that either other WNT proteins or other compensatory pathways are involved in this process of brain development in humans.

In these four families, biallelic mutations in *WNT1* resulted in a moderately severe and progressive OI phenotype that is indistinguishable from dominant OI type III. The *WNT1* mutations we identified in 10.5% of our 38 previously unsolved OI cases are not present in the NHLBI EVS or in dbSNP. As noted above, the mutation identified in the Hmong family was detected in another family from the same region by another group. In three of the families, the affected individuals also have learning and developmental delays, but we are uncertain of the status in the fourth family. As a result, it is not yet clear whether these neurologic abnormalities are part of the clinical phenotype that results from mutations in *WNT1* or whether they are due to other factors. As more families are identified, this should become more clear. Although the precise mechanisms by which mutations in *WNT1* result in OI have not yet been defined, these findings should lead to a more detailed analysis of the role of the gene product in bone development, stabilization, and

structure and might provide another OI subset in which targeted treatment could be effective.

Acknowledgments

This work was supported in part by funds from the Osteogenesis Imperfecta Foundation (Michael Geisman Fellowship to S.M.P.), the Northwest Institute for Genetic Medicine and the Washington State Life Sciences Discovery Fund (grant 265508), the Freudmann Fund for Translational Research at the University of Washington, and research funds from the Department of Pathology, University of Washington. We are grateful to Brendan Lee and his collaborators for discussing their work with us prior to publication and for allowing us to cite the work to share credit for the recognition that *WNT1* mutations play a role in recessive forms of osteogenesis imperfecta.

Received: December 31, 2012
Revised: February 7, 2013
Accepted: February 14, 2013
Published: March 14, 2013

Web Resources

The URLs for data presented herein are as follows:

dbSNP, http://www.ncbi.nlm.nih.gov/projects/SNP/
NHLBI Exome Sequencing Project (ESP) Exome Variant Server, http://evs.gs.washington.edu/EVS/
Online Mendelian Inheritance in Man (OMIM), http://www.omim.org/
RefSeq, http://www.ncbi.nlm.nih.gov/RefSeq
SeattleSeq Annotation 137, http://snp.gs.washington.edu/SeattleSeqAnnotation137/

References

1. Lapunzina, P., Aglan, M., Temtamy, S., Caparrós-Martín, J.A., Valencia, M., Letón, R., Martínez-Glez, V., Elhossini, R., Amr, K., Vilaboa, N., and Ruiz-Perez, V.L. (2010). Identification of a frameshift mutation in Osterix in a patient with recessive osteogenesis imperfecta. Am. J. Hum. Genet. *87*, 110–114.
2. Morello, R., Bertin, T.K., Chen, Y., Hicks, J., Tonachini, L., Monticone, M., Castagnola, P., Rauch, F., Glorieux, F.H., Vranka, J., et al. (2006). CRTAP is required for prolyl 3- hydroxylation and mutations cause recessive osteogenesis imperfecta. Cell *127*, 291–304.
3. Barnes, A.M., Chang, W., Morello, R., Cabral, W.A., Weis, M., Eyre, D.R., Leikin, S., Makareeva, E., Kuznetsova, N., Uveges, T.E., et al. (2006). Deficiency of cartilage-associated protein in recessive lethal osteogenesis imperfecta. N. Engl. J. Med. *355*, 2757–2764.
4. Cabral, W.A., Chang, W., Barnes, A.M., Weis, M., Scott, M.A., Leikin, S., Makareeva, E., Kuznetsova, N.V., Rosenbaum, K.N., Tifft, C.J., et al. (2007). Prolyl 3-hydroxylase 1 deficiency causes a recessive metabolic bone disorder resembling lethal/severe osteogenesis imperfecta. Nat. Genet. *39*, 359–365.
5. Baldridge, D., Schwarze, U., Morello, R., Lennington, J., Bertin, T.K., Pace, J.M., Pepin, M.G., Weis, M., Eyre, D.R., Walsh, J., et al. (2008). CRTAP and LEPRE1 mutations in recessive osteogenesis imperfecta. Hum. Mutat. *29*, 1435–1442.
6. van Dijk, F.S., Nesbitt, I.M., Zwikstra, E.H., Nikkels, P.G., Piersma, S.R., Fratantoni, S.A., Jimenez, C.R., Huizer, M., Morsman, A.C., Cobben, J.M., et al. (2009). PPIB mutations cause severe osteogenesis imperfecta. Am. J. Hum. Genet. *85*, 521–527.
7. Barnes, A.M., Carter, E.M., Cabral, W.A., Weis, M., Chang, W., Makareeva, E., Leikin, S., Rotimi, C.N., Eyre, D.R., Raggio, C.L., and Marini, J.C. (2010). Lack of cyclophilin B in osteogenesis imperfecta with normal collagen folding. N. Engl. J. Med. *362*, 521–528.
8. Pyott, S.M., Schwarze, U., Christiansen, H.E., Pepin, M.G., Leistritz, D.F., Dineen, R., Harris, C., Burton, B.K., Angle, B., Kim, K., et al. (2011). Mutations in PPIB (cyclophilin B) delay type I procollagen chain association and result in perinatal lethal to moderate osteogenesis imperfecta phenotypes. Hum. Mol. Genet. *20*, 1595–1609.
9. Christiansen, H.E., Schwarze, U., Pyott, S.M., AlSwaid, A., Al Balwi, M., Alrasheed, S., Pepin, M.G., Weis, M.A., Eyre, D.R., and Byers, P.H. (2010). Homozygosity for a missense mutation in SERPINH1, which encodes the collagen chaperone protein HSP47, results in severe recessive osteogenesis imperfecta. Am. J. Hum. Genet. *86*, 389–398.
10. Alanay, Y., Avaygan, H., Camacho, N., Utine, G.E., Boduroglu, K., Aktas, D., Alikasifoglu, M., Tuncbilek, E., Orhan, D., Bakar, F.T., et al. (2010). Mutations in the gene encoding the RER protein FKBP65 cause autosomal-recessive osteogenesis imperfecta. Am. J. Hum. Genet. *86*, 551–559.
11. Shaheen, R., Al-Owain, M., Faqeih, E., Al-Hashmi, N., Awaji, A., Al-Zayed, Z., and Alkuraya, F.S. (2011). Mutations in FKBP10 cause both Bruck syndrome and isolated osteogenesis imperfecta in humans. Am. J. Med. Genet. A. *155A*, 1448–1452.
12. Homan, E.P., Rauch, F., Grafe, I., Lietman, C., Doll, J.A., Dawson, B., Bertin, T., Napierala, D., Morello, R., Gibbs, R., et al. (2011). Mutations in SERPINF1 cause osteogenesis imperfecta type VI. J. Bone Miner. Res. *26*, 2798–2803.
13. Becker, J., Semler, O., Gilissen, C., Li, Y., Bolz, H.J., Giunta, C., Bergmann, C., Rohrbach, M., Koerber, F., Zimmermann, K., et al. (2011). Exome sequencing identifies truncating mutations in human SERPINF1 in autosomal-recessive osteogenesis imperfecta. Am. J. Hum. Genet. *88*, 362–371.
14. Martínez-Glez, V., Valencia, M., Caparrós-Martín, J.A., Aglan, M., Temtamy, S., Tenorio, J., Pulido, V., Lindert, U., Rohrbach, M., Eyre, D., et al. (2012). Identification of a mutation causing deficient BMP1/mTLD proteolytic activity in autosomal recessive osteogenesis imperfecta. Hum. Mutat. *33*, 343–350.
15. Asharani, P.V., Keupp, K., Semler, O., Wang, W., Li, Y., Thiele, H., Yigit, G., Pohl, E., Becker, J., Frommolt, P., et al. (2012). Attenuated BMP1 function compromises osteogenesis, leading to bone fragility in humans and zebrafish. Am. J. Hum. Genet. *90*, 661–674.
16. Shaheen, R., Alazami, A.M., Alshammari, M.J., Faqeih, E., Alhashmi, N., Mousa, N., Alsinani, A., Ansari, S., Alzahrani, F., Al-Owain, M., et al. (2012). Study of autosomal recessive osteogenesis imperfecta in Arabia reveals a novel locus defined by TMEM38B mutation. J. Med. Genet. *49*, 630–635.
17. Bernier, F.P., Caluseriu, O., Ng, S., Schwartzentruber, J., Buckingham, K.J., Innes, A.M., Jabs, E.W., Innis, J.W., Schuette, J.L., Gorski, J.L., et al.; FORGE Canada Consortium. (2012). Haploinsufficiency of SF3B4, a component of the pre-mRNA spliceosomal complex, causes Nager syndrome. Am. J. Hum. Genet. *90*, 925–933.

18. Li, H., and Durbin, R. (2009). Fast and accurate short read alignment with Burrows-Wheeler transform. Bioinformatics *25*, 1754–1760.
19. Janda, C.Y., Waghray, D., Levin, A.M., Thomas, C., and Garcia, K.C. (2012). Structural basis of Wnt recognition by Frizzled. Science *337*, 59–64.
20. Doubravska, L., Krausova, M., Gradl, D., Vojtechova, M., Tumova, L., Lukas, J., Valenta, T., Pospichalova, V., Fafilek, B., Plachy, J., et al. (2011). Fatty acid modification of Wnt1 and Wnt3a at serine is prerequisite for lipidation at cysteine and is essential for Wnt signalling. Cell. Signal. *23*, 837–848.
21. Willert, K., and Nusse, R. (2012). Wnt proteins. Cold Spring Harb. Perspect. Biol. *4*, a007864.
22. van Noort, M., Meeldijk, J., van der Zee, R., Destree, O., and Clevers, H. (2002). Wnt signaling controls the phosphorylation status of beta-catenin. J. Biol. Chem. *277*, 17901–17905.
23. Heo, J.S., Lee, S.Y., and Lee, J.C. (2010). Wnt/β-catenin signaling enhances osteoblastogenic differentiation from human periodontal ligament fibroblasts. Mol. Cells *30*, 449–454.
24. Fujita, K., and Janz, S. (2007). Attenuation of WNT signaling by DKK-1 and -2 regulates BMP2-induced osteoblast differentiation and expression of OPG, RANKL and M-CSF. Mol. Cancer *6*, 71.
25. Gong, Y., Slee, R.B., Fukai, N., Rawadi, G., Roman-Roman, S., Reginato, A.M., Wang, H., Cundy, T., Glorieux, F.H., Lev, D., et al.; Osteoporosis-Pseudoglioma Syndrome Collaborative Group. (2001). LDL receptor-related protein 5 (LRP5) affects bone accrual and eye development. Cell *107*, 513–523.
26. Boyden, L.M., Mao, J., Belsky, J., Mitzner, L., Farhi, A., Mitnick, M.A., Wu, D., Insogna, K., and Lifton, R.P. (2002). High bone density due to a mutation in LDL-receptor-related protein 5. N. Engl. J. Med. *346*, 1513–1521.
27. Little, R.D., Carulli, J.P., Del Mastro, R.G., Dupuis, J., Osborne, M., Folz, C., Manning, S.P., Swain, P.M., Zhao, S.C., Eustace, B., et al. (2002). A mutation in the LDL receptor-related protein 5 gene results in the autosomal dominant high-bone-mass trait. Am. J. Hum. Genet. *70*, 11–19.
28. Niziolek, P.J., Farmer, T.L., Cui, Y., Turner, C.H., Warman, M.L., and Robling, A.G. (2011). High-bone-mass-producing mutations in the Wnt signaling pathway result in distinct skeletal phenotypes. Bone *49*, 1010–1019.
29. Liu, G., Vijayakumar, S., Grumolato, L., Arroyave, R., Qiao, H., Akiri, G., and Aaronson, S.A. (2009). Canonical Wnts function as potent regulators of osteogenesis by human mesenchymal stem cells. J. Cell Biol. *185*, 67–75.
30. Malhotra, S., and Kincade, P.W. (2009). Wnt-related molecules and signaling pathway equilibrium in hematopoiesis. Cell Stem Cell *4*, 27–36.
31. Kramer, I., Halleux, C., Keller, H., Pegurri, M., Gooi, J.H., Weber, P.B., Feng, J.Q., Bonewald, L.F., and Kneissel, M. (2010). Osteocyte Wnt/beta-catenin signaling is required for normal bone homeostasis. Mol. Cell. Biol. *30*, 3071–3085.
32. Karsenty, G., and Wagner, E.F. (2002). Reaching a genetic and molecular understanding of skeletal development. Dev. Cell *2*, 389–406.
33. McMahon, A.P., and Bradley, A. (1990). The Wnt-1 (int-1) proto-oncogene is required for development of a large region of the mouse brain. Cell *62*, 1073–1085.
34. Thomas, K.R., Musci, T.S., Neumann, P.E., and Capecchi, M.R. (1991). Swaying is a mutant allele of the proto-oncogene Wnt-1. Cell *67*, 969–976.